FLUCOME 2009
10th International Conference on Fluid Control, Measurements, and Visualization
August 17–21, 2009, Moscow, Russia

VISUALIZATION OF STRATIFIED AND ROTATING FLOWS FINE STRUCTURE

Yuli D. Chashechkin[1]

ABSTRACT

Visualization by sensitive optic methods namely schlieren and shadow as well as electrolytic precipitation and dyeing are widely used for stratified flows. Conditions of experiment completeness and adequacy are discussed. Bright colour schlieren images of the flow are produced using 'natural rainbow method' exploring refraction and dispersion of a light in the fluid. Wide view field and a high spatial resolution of schlieren instruments allow observing simultaneously large and small scale flow components. General features of substances transportation in stratified and vortex flows are marked. Streaky structures in flows are identified and their transformation into vortex system is registered. Anisotropic transport of a dye in a compound vortex contacting a free surface is registered.

Keywords: stratification, Schlieren instrument, light dispersion, colour image, fine structure.

INTRODUCTION

It is well known that remote-sensing techniques, including shadowgraphs, schlieren and interferometry developed for astronomic optics testing and visualization of compressible gas flows, are used for studying a stratified liquid flows. Changes in concentration, temperature and density of a fluid are accompanied by variations in refractive index. Disturbances of the refractive index, which are large enough in liquids, produce changes in the schlieren images. The application of optic methods for stratified flows visualization is extended by using effects of light dispersion and refraction of the light rays even in the undisturbed medium. A tank with the vertical wall filled with stratified brine is similar to an optical prism. The optic length of the light ray is determined by the refractive index profile for a constant geometric width of the tank. Moreover in a stratified liquid all the changes in reflected index are many times greater than those encountered in compressible gas flows. That is why the conventional visualization instruments (interferometer, schlieren, shadow) cannot be used directly for stratified flows studies and should be specially tuned.

In practice different modifications of schlieren methods proposed by D.D. Maksoutov (1934) are used in view of their sensitivity, flexibility and universality. A common schlieren instrument consists of two separate illuminating and receiving parts. Each part contains an objective consisting of a main mirror and a compensating meniscus to compensate aberrations of the set. Maksoutov's schlieren instrument consists of two similar objectives and their asymmetric aberrations are mutually compensated during assembling and adjustment. Another very important Maksoutov's improvement is replacing of a circular illuminating

[1] Corresponding author: Institute for Problems in Mechanics of the RAS, e-mail: chakin@ipmnet.ru

diaphragm, the conventional source of light for optical measurements, by an elongated illuminating slit. To produce the schlieren effect part of the light forming the image of the light source must be cut off in the receiving part. Besides a sharp blade edge (the Foucault knife), several kinds of light cutting diaphragms, specifically, a thin filament, a narrow slit between two blade edges or a graded schlieren filter for closing part of light rays have been proposed by Maksoutov (1934). Due to a mean deflection and dispersion of light in a stratified liquid the action of cutting diaphragm depends on angular positions of the illuminating slit and of the cutting diaphragm in the focal planes.

Flexible Maksoutov's method can also be used for producing a 'natural rainbow' image of a stratified flow. The objective of this paper is to present a short theory of this schlieren instrument taking into account the dispersion of light, to describe a simple modification of the traditional schlieren instrument enlarging its dynamic range and to give examples of colour patterns, visualizing all well-known conventional and some new components of flows. Effects of fine flow components on anisotropic transportation of a solvable dye observed in some stratified and rotating flows are discussed briefly.

THEORETICAL BACKGROUND

Interpretation of flow visualization patterns depends of basic flow model, which is based on complete set of exact solution of set of fundamental governing equations. The set includes equation of state by Mendeleev, characterizing physical properties of the medium, and differential equations of continuity by D'Alembert, transport of momentum by Navier-Stokes, heat by Fourier and stratified substances by Fick. The system of governing equations is singular disturbed type system of a high order due to smallness of kinetic coefficients and density changes. Complete solution of such sets includes both regular disturbed and singular disturbed on small coefficients functions. Classification of linearized fundamental set solutions is given by Chashechkin and Kistovich (2007). Properties of large-scale regular disturbed flow components (*redics*) and thin singular disturbed flow components (*sidics*) are discussed. Well-known flow components that are waves, vortices, jets, and wakes form a set of *redics*. Set of *sidics* is richer than the set of *redics* and includes families of Stokes type boundary layers on a free surface and solid boundaries as well as their analogues in a fluid interior as shown by Chashechkin (2007).

Length scales of *redics* are defined by flow geometry, kinematic and stratification value. Scale of stratification is inverse logarithmic derivative $\Lambda = \left| d \ln \rho / dz \right|^{-1}$ of density ρ. Typical time scale of stratified flow is buoyancy period T_b and frequency $N = 2\pi / T_b = \sqrt{g / \Lambda}$, $\mathbf{g}$ is gravity acceleration. Sizes of obstacles L and internal wave-lengths λ ($\lambda = UT_b$ for attached (lee) waves produced by flow on an obstacle moving with velocity U) form a set of *macroscopic* length scales. Ratio of geometric and viscous-wave length-scales $L_\nu = \sqrt[3]{g\nu}/N$ (ν is kinematic viscosity) characterizes modal structure of the wave fields as shown by Chashechkin (2007).

Transverse scales of singular disturbed components (s*idics*) are characterized by universal micro-scales defined by buoyancy frequency N and/or general flow rotation frequency Ω. Micro-scale lengths for velocity fields of Stokes like boundary layers are $\delta_N = \sqrt{\nu / N}$ or $\delta_\Omega = \sqrt{\nu/\Omega}$ and for Prandtl's boundary layer is $\delta_u = \nu/U$, for temperature and salinity (density) fields are $\delta_T = \sqrt{\kappa_T / N}$, $\delta_S = \sqrt{\kappa_S / N}$. Due to smallness of kinetic coefficients transverse sizes of *sidics* are small and for their visualization the most sensitive well spatially resolved methods had to be used. *Redics* characterize field of momentum and energy. *Sidics* are responsible of vorticity field and it transportation, large vortex formation and non-uniform transport of substances in flows. In limiting case of homogeneous fluid approximation different sidics become identical and are merged. In this approximation the set of governing equations become degenerated on singular disturbed components.

EXPERIMENTAL SETUP

Schemes of experimental sets-up are shown in Fig. 1. Side view of stratified flows is visualized by mirror schlieren instrument IAB-458 *1 – 12*. Optical system consists of separate illuminating and receiving parts and includes white light source *1*; condenser *2*, forming image of the light source in plane of illuminating diaphragm; lighting slit *3*; plane turning mirrors *4*, *9*, directing light rays on main spherical mirrors *5*, *8*; meniscus *6*, *7* correcting aberrations; light cutting diaphragm *10* (filament, Foucault's knife or regular grating is forming schlieren effect), lens *11*, constructing image of the flow pattern in camera *12*. Diameter of the observation field is 23 cm and is large enough to observe regular flow components. The spatial resolution of the used schlieren instrument is better than 0.1 mm (Chashechkin, 1999).

Experiments are performed in a rectangular tank *15* $70\times25\times70$ cm^3 with side windows *14* filled with linearly stratified brine through the bottom valve *15* using of the two-tank *13* method. The flow is observed by the Schlieren instrument IAB-458 through the optical windows *14*.

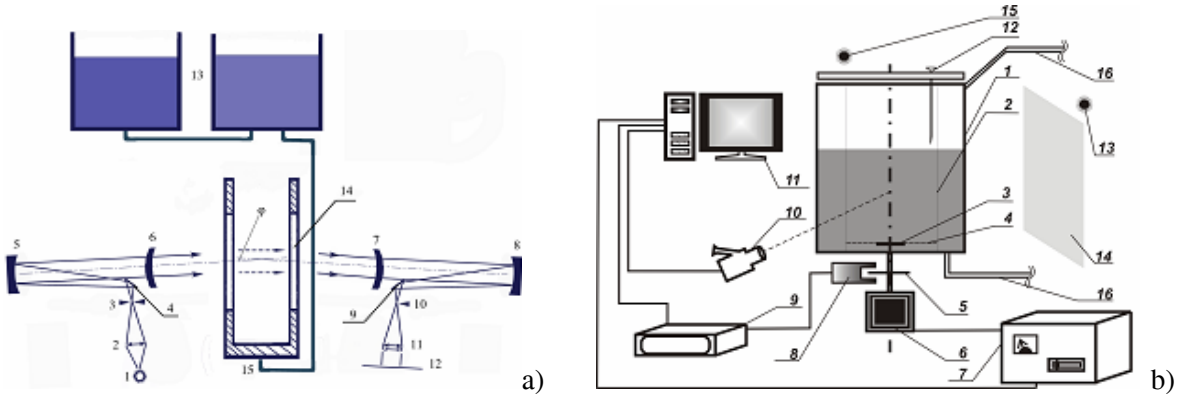

Fig. 1. Schemes of experimental sets-up:
***a*) – for visualization of stratified flows and *b*) – for compound vortex flows.**

Scheme of set-up for visualization of compound vortex flows are presented in Fig. 1, *b*. In rectangular Perspex tank *1* of length 59 cm, width 41 cm and height 70 cm a Perspex cylindrical chamber *2* of internal diameter 29.4 cm is placed. The rotating disk *3* of diameter 5, 10, 15 and 29 cm is placed on the bottom of the chamber *2* The bottom *4* of the chamber with the disk is flat. Disk is driven into motion by electric motor 6, operated by controller 7. Working range of rotation frequency is ranged from 200 to 2500 revo. Disk with transparent mask *5* is used to measure rotation speed by means of counter *8* and register *9*. Flow pattern is registered with photo- or video camera *10*. Experiment is controlled by computer *11*. Dye is introduced on the surface or in a fluid interior by dosing dropper *12*. Flow pattern is uniformly illuminated by white light source *13* through dispersive sheet *14*. Lamp of UF-light *15* is used for illumination of fluorescent dye. Both tank and chamber are filled with degassed tap water through hydraulic system *16*.

After filling the tank disk 3 was put into rotation at given rotation frequency and started to swirl and pump a fluid into the chamber. After finishing of all the transfer processes and formation of stable flow pattern the shape of surface trough was registered. Then 0.1 ml drop of dye was introduced by dosing dropper in selected point on the surface. Diluted blue or black ink and solution of Uranil were used for flow visualization, as indicated in the work by Stepanova and Chashechkin (2008). Experimental data were processed by standard software.

EXPERIMENTAL RESULTS

Redics and sidics in stratified flow past a uniformly moving horizontal strip and cylinder are visualized by schlieren instrument and shown in Fig. 2. Diffusive colour curves visualize crests and troughs of lee internal waves that are redics of the flow. Near the strip of length L_c = 2.5 cm uniformly moving with velocity U = 2.3 cm/s from right to left set of sidics forms a transverse streaky wake shown in Fig. 2. The leading edges of separate streaks are directed horizontally, while their sharp outer edges are oriented almost vertically. The streaky wake remains rather narrow due to the buoyancy forces suppressing the vertical displacement of fluid particles. Due to the shear flow inside the velocity wake, the streaks elongate in the horizontal direction. They are gradually smoothed by molecular diffusion and disappear.

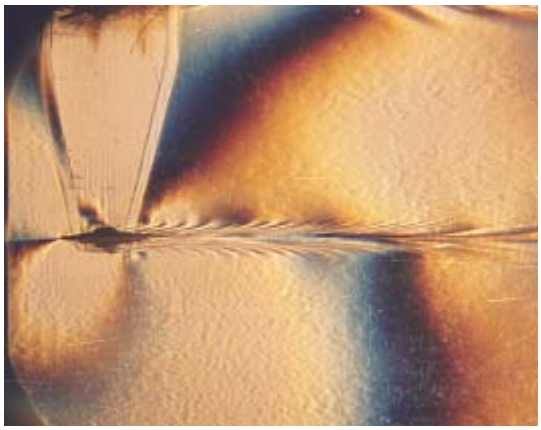

a)

b)

Fig. 2. Pattern of flow around strip moving from right to left ("slit-thread" method); T_b = 7.5 s, L_c = 2.5 cm; *a*, *b*) – U = 2.3; 1.4 cm/s, $\alpha = 0$; 12.5°.

The lift force changes the flow pattern around the sloping strip. If the first trough and first crest in Fig. 2, *b* is located, respectively, at the strip leading edge in upper semi-space and the strip rear edge in lower semi-space, the next troughs in the both semi-spaces contact each other through the thin density wake. The central interface of the wake becomes wavy-shaped with a spatial period equal to the length of the attached internal waves $\lambda = U \cdot T_b$. In the upper semi-space, the streaks in the upwind side of the obstacle are arranged with relatively large intervals. They separate only from the rear edge of the strip.
As a contrast, in the downwind strip side the streaky structure separates along the entire surface, starting the leading edge of the strip. The overall length of the domain occupied by the streaky structures and thickness of individual interfaces are the same, however, the total numbers of sloping interfaces are different in the upper and lower hemi-spaces, respectively. Due to the baroclinicity, this domain is characterized by high level of vorticity existing in the form of superposed interfaces.

Subsequent evolution of the flow structure, when increasing the strip velocity, is presented in Fig. 3. At a moderate velocity the wave pattern is antisymmetric and the trough marked by curve grey line in upper hemi-space contacts with the crest in lower hemi-space that is marked by deep-blue curve. The pattern of the streaky structures is symmetric both in general and in individual details. The separating streaks extend horizontally with the distance from the obstacles and then gradually disappear (Fig. 3, *a*). With the body velocity increase the streaky patterns keep the symmetry. They are arranged separately with some interval between themselves.

Sufficiently far from the strip, symmetric pairs of the streaks transform into a butterfly-like structure, presented in Fig. 3 *b*. In vicinity of the central horizontal plane, a sharp pattern with thin interfaces near the body gradually turns, with the distance from the obstacle, to blur due to overlapping of

slightly sloping interfaces. Separate interfaces lost their plane form and become wavy in the spanwise direction. The outer edges of the streaky structures are connected between themselves with long interfaces oriented almost horizontally. The maximum vertical size of the wake is within 0.4 cm.

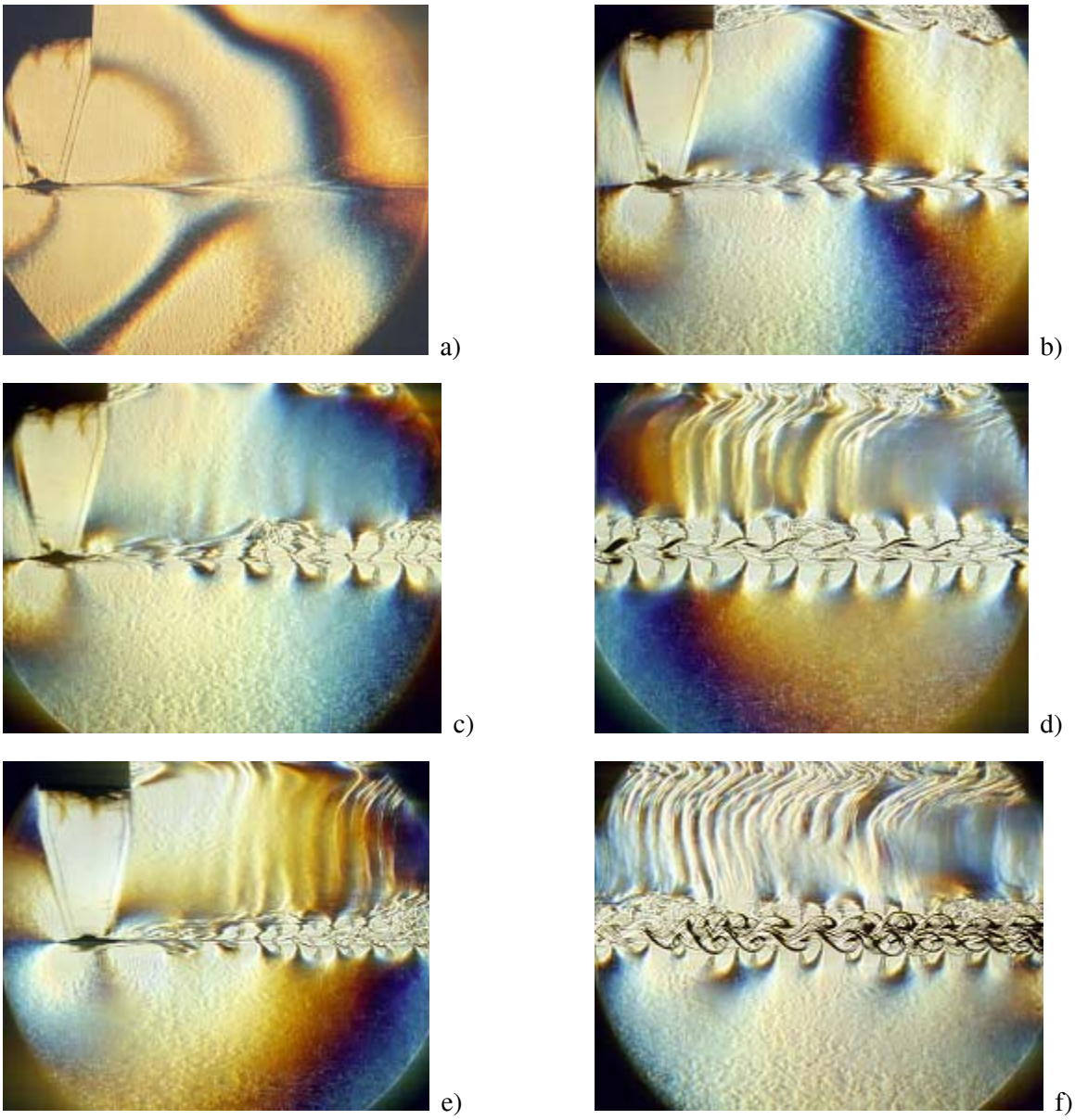

Fig. 3. Evolution of the flow pattern around the horizontal strip moving from right to left with the velocity increase, L_b = 2.5 cm T_b = 7.5 s; *a-f*) – U = 1.38; 3.2; 4.9; 4.9; 5.25; 5.25 cm/s, "slit-thread" method.

Substantially more complex structure is presented in Fig 3, *c*, *d* where two sequential photos of the same experiment illustrate evolution of flow pattern vs time, or vs distance from the strip, $x = U \cdot t$. Near the body the elongated interfaces exist, the density wake is symmetric and arranged horizontally. Next, the trailing edges of the separate interfaces are reconnected and the butterfly-like vortices are formed. The leading and trailing edges of these spanwise elongated vortices move in opposite directions and distort the shape of the wake. The wake central part becomes wavy. Vertical motions enhance the density variations,

so the sloping interfaces inside the density wake come into particular pronounced and are visualized by short sloping black lines near the central plane in Fig. 3 *d*. The vertical motion is insensibly suppressed by stratification and fluid particles relax to their neutral buoyancy horizons. As a result, the interfaces inside the density wake are oriented almost horizontally.

With further strip velocity increase, a general structure of the flow is conserved, but the lengths of detailed component vary. Several elongated streaky structures are observed in Fig. 3, *e* on the strip sides and in the near downstream wake. With the distance, the sharp central interface past the strip starts to oscillate and, near the turning points, the vortices gradually form a set of smooth butterfly-like disturbances, and further the ones having the sharp interfaces inside. With an increase of the wake wavy oscillations the central plane interface of the downstream wake splits into a set of interfaces. The flow come into wavy form both in longitudinal and in the spanwise direction. In the complex pattern of flow shown in Fig. 3, *f* several sets of vortices are distinguished in spanwise direction that is along the ray of observation. The flow past the 2D strip includes 3D vortex structure and gradually decays into set of interfaces. Intensively moving 3D vortices produce a number of secondary internal waves outside the density downstream wake. Their length and slope are determined by the size and relative translation velocity of a forming vortex.

Fig. 4. Pattern of flow around a vertical strip with H_c = 2.5 cm moving from right to left: *a*, b) – T_b = 12.5 s, U = 0.1 cm/s; "slit-thread" and "slit-knife" methods; c) – T_b = 17.4 s, U = 0.3 cm/s, "slit-knife" method.

To illustrate a degree of the flow pattern reproducibility, two first images shown in Fig. 4 present the same flow pattern produced by vertical strip of height H_c = 2.5 cm moving uniformly in horizontal direction , visualized by the two schlieren methods in different experiments. Comparison of images in Fig. 4, *a* and Fig. 4, *b* shows that different fine structural elements are reproduced one-to-one in independent experiments. An increase of the interfaces lengths in Fig.4, *a*, comparably to Fig. 4, *b*, is due to a higher sensitivity of conventional schlieren method under the given conditions of the instrument tuning. The curved dark and light strips visualising attached internal wave past the body are imperfect circular arcs that is caused by the Doppler effect inside the velocity wake shear flow.

The vertical markers indicate a profile of the velocity horizontal component. An upstream central jet representing blocked fluid is pronounced in more extent than the downstream wake. The height of the velocity wake exceeds the density wake thickness bounded by two sloping interfaces. The density wake wedge contacts the vertical strip through the single central interface whose length is about 2 cm. The sharp edges of the strip generate their own set of upstream disturbances. Short black and white lines near the strip edges in Fig.4, *a*, indicate the areas of maximum density gradient.

With the velocity increase, the vorticity is accumulated in the rear part of the obstacle. The stationary symmetric rear vortex past the vertical strip in Fig.4, *c*, is bounded by high gradient envelope separated from the strip edges. The shedding of eddies from the rear vortices pair is suppressed by attached internal waves, so wake past the obstacle is thin. Further the wake expands following the phase structure of the internal waves. After the first expansion, interfaces are arranged almost horizontally.

Shapes of the intensive attached internal waves are only slightly disturbed by the shear downstream flow at this regime.

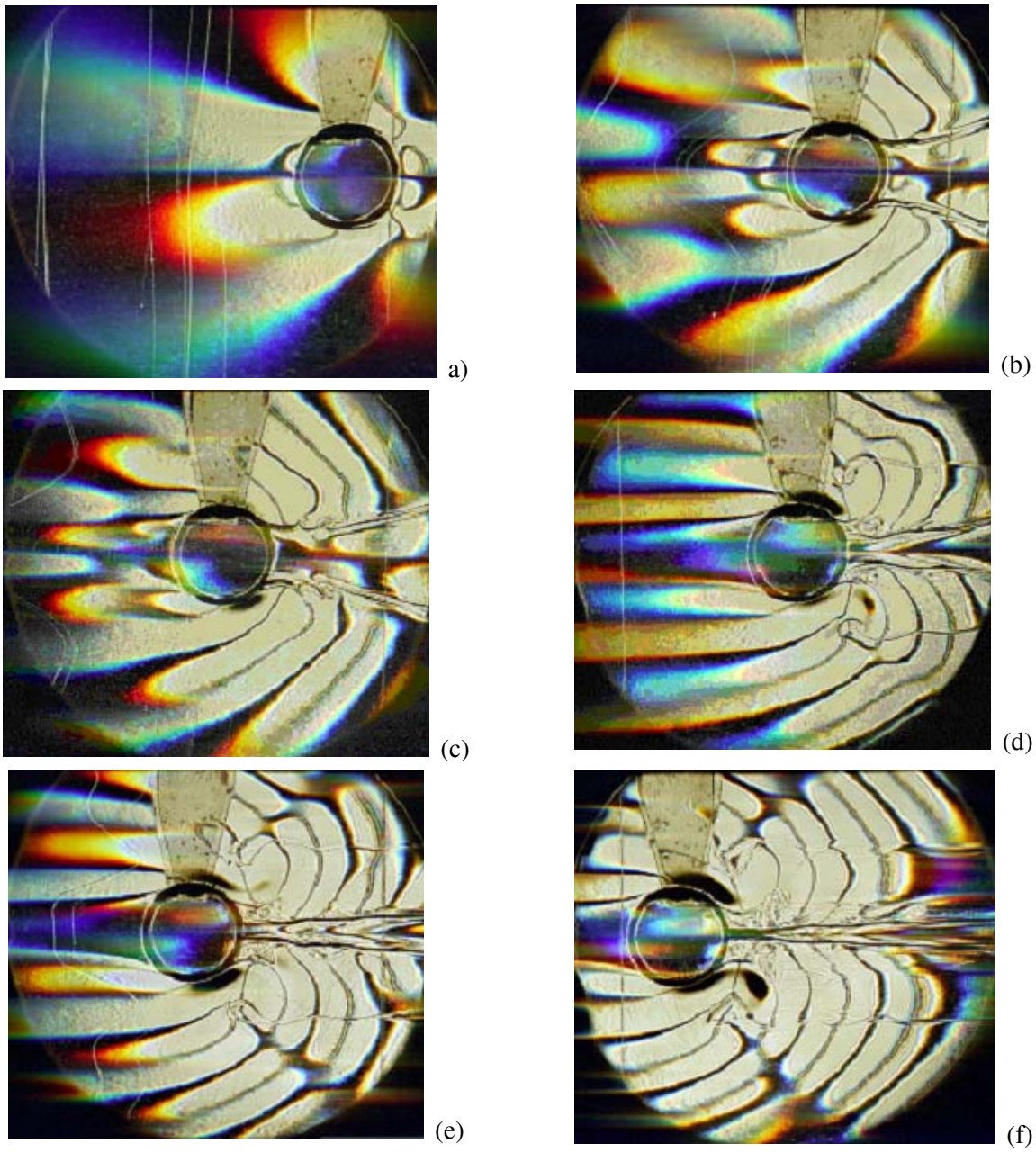

Fig. 5. Soaring interfaces and vortices in flow pattern past the horizontally moving cylinder in the stratified fluid ($D = 5$ cm, $T_b = 10.5$ s, $U = 0.24$ cm/s) at different times after beginning of the motion; *a-f)* – $\tau = t / T_b =$ 0.6; 1,9; 2.9; 8.1; 11,9; 17.1. Thin initially vertical and then disturbed lines in Fig. 5 a –c and e are density markers produced by free falling sugar crystals visualizing fluid velocity profiles.

New features of the past horizontal cylinder that are soaring interfaces (soaring sidics) which are transformed with time into soaring vortex systems are visualized by effective method 'vertical slit-thin filament in focus'. Disturbed vertical lines in Fig. 5, *a-c*, *e* are density markers. Their shapes show that

transient velocity disturbance is smooth on all horizons. Formation of completely blocked fluid (deep blue band) ahead of the cylinder leads to flat part in the profile of displacements where fluid and the body velocities are equal Fig. 5, *e*. Complex structure of upstream domain in Fig. 5, *b* and *c*, shows that there are several groups of transient disturbances running ahead during the process of liquid blocking. The latest portion of disturbances is bounded by high gradient interfaces marking the boundaries of blocked fluid.

The size of soaring vortex structure and intensity of vortex motion in this regime are small as wave amplitudes are not very large in this regime. In vicinity of dark sloping lines in Fig. 5, *e*, *f* waves from inner region contact on the soaring interfaces the waves from outer region in antiphase. At the stage of the soaring interfaces formation crests from inner wave zone and troughs from outer wave zone contact in vicinity of the soaring interfaces (Fig. 5, *d*), but with time this area become more pronounced. This line can be identified in Fig. 5, *e*, *f* as outer boundary of domain of closed elliptic isopleths, and as boundary of regular outer waves. Oscillating character of soaring interfaces indicate amplitudes of vertical displacements inside wave field. Shapes of vortices immersed in the wake and formation of strong density gradient near the downstream wake central plane indicate properties of vortex motion in this region. Broken lines in the domains of intersections of wave crests, troughs and interfaces past the soaring vortex manifest existence of very narrow current and high gradients interface here.

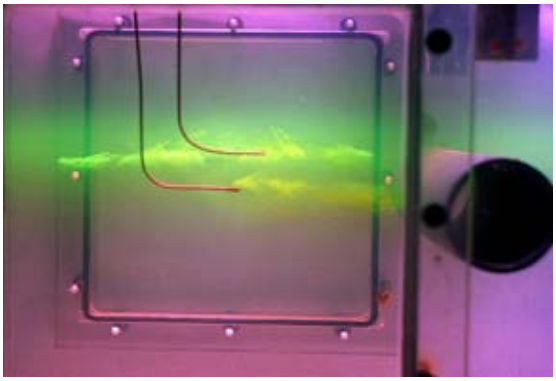
a)

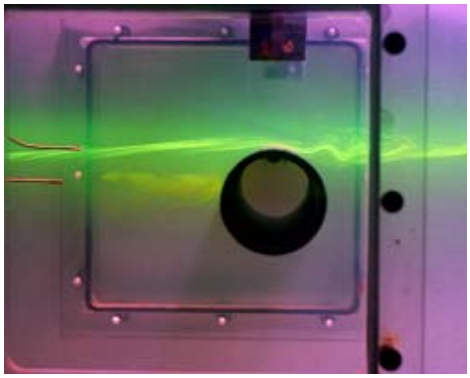
b)

Fig. 6. Reforming of the dye patches by the cylinder moving from right to left ($D = 7.6$ **cm;** $T_b = 7.1$ **s;** $U = 0.24$ **cm/s): *a*, *b*) –** $\tau =$ **0, 7.4.**

Due to specific organization of the flow the interfaces act as accumulator of passive admixture. Evolution of dye patches coloured motionless water in the tank (Fig. 6, *a*) depends on their initial positions. After beginning of the motion part of unchanged cloud of the dye is transported along with the blocked fluid ahead of the cylinder center. Part of the dye overflows the cylinder and accumulated in the downstream wake in bright strips coinciding with high-gradient interfaces in schlieren images of the similar undyed flows (Fig. 6, *b*). Shape of bright interface past the cylinder are waved by lee internal waves. Dimensionless time $\tau = t / T_b$ is counted from beginning of the body motion. Due to analogy between stratified and rotating flows anisotropic transport of a dye manifest itself in vortex flows too.

ANISOTROPIC TRANSPORT OF A DYE IN COMPOUND VORTEX

Details of experiment with a dye transport by compound vortex produced by rotating disc in the cylindrical chamber are shown in Fig. 7, a. Photo of the dye extracted from coloured spots was done by the digital photo camera Canon EOS 350D (line of view is directed from above on a free surface under the angle of 30˚ to the vertical axis). The white and UV light sources are placed above the tank to observe the Uranil solution conserved on the liquid surface. Dye inside the fluid is almost invisible under this illumination. Fluid involved into compound vortex motion in a cylindrical chamber 1 forms circular

contact line 2. Far circular line 3 is the contact line of cylindrical chamber with transparent bottom of tank. Fluid is driven by uniformly rotating transparent disk, with marked outer edge 4. The metal pivot 5 connecting disk with the electro motor is visible. The silk filaments 6 show the fluid is involved into cyclonic rotation (in counter-clockwise direction) marked by two black arrows. The dye extracted from the central spot form spiral strip 7 with a sharp tip moving along the surface of rotating fluid in clockwise direction (anti-cyclonic propagation). Black arrow near the spiral arm indicates direction of the dye spiral tip propagation. The fluid generally rotates in counter clockwise direction. The surface pattern of dye rotates together with the fluid. The tip of the arm moves in opposite clockwise direction. The tip goes away from the central axis of rotation and ascends along the surface trough.

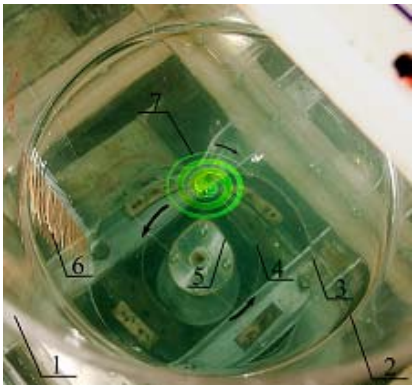

a)

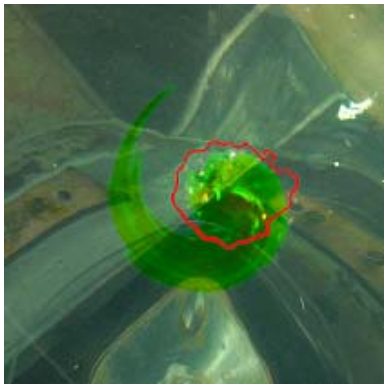
b)

Fig. 7. Spiral arm of uranil arising from the central spot at free surface: *a, b)* – general view and initial phase of the dye spot deformation ($H = 40$ cm, $\Omega = 200$ RPM, $R = 7.5$ cm).

General transformation of the initial round dye spot into sharpen spiral is illustrated in Fig. 7, *a* where superimposed images are shown. Red line in the Fig. 7, *b* marks the initial boundary of the Uranil spot deformed by small vortices formed in thin layer between the spot with zero tangential velocity and surrounding rotating fluid. These small scale vortices are damped very fast. The comma-like spiral arm with a heavy head and sharp tip is gradually extracted from the round dye spot (Fig. 7, *b*).

Evolution of the dye spot form on the rotating free surface is shown in Fig. 8 (photos presented in the both Fig. 7 and Fig. 8 are captured during the same experiment). Initial drop having only vertical component of velocity falls on the rotating fluid surface and starts to spin up by rotating fluid. Wavy deformation of the spot edge in Fig. 8, *a* illustrate impact of small vortices forming in the shear layer between quiescent spot and rotating fluid during the initial stage of the dye spot spin up process. The average size of vortices is 3.8 mm. With time small vortex motion decays and one spiral arm starts to grow from smooth round spot (Fig. 8, *b*). The concentration of the dye is strongly nonuniform in the arm. Bright extended filaments are separated by darker domains of lower concentration of the dye (Fig. 8, *c*).

The sharp tip of the arm is extended in the clockwise direction whereas the fluid body rotates in counterclockwise direction. The behavior of the dye reflects a deficit of angular momentum in falling drop. The deficit of momentum is conserved and that explains the dye movement in direction opposite to the general rotation. The spinning of the dye from the central spot continues with time (Fig. 8, *b*, *c*).

Spinning of the dye into thin filament competes with the uniform enlarging of the dye spot under isotropic diffusion action. Formation of thin filament from large round spot manifests complex structure of the vortex motion. The compound vortex consists of smooth large scale rotation and embedded small scale motions. With time the number of coils in the spiral arm is gradually increasing (Fig. 8, c). The width of the arm is gradually increasing from 0.70 mm near the sharp tip to 1.08 cm in region of contact with the spot. The width of the free of dye band gradually decreases with time. Similar features of the dye transport were observed in stratified flows earlier.

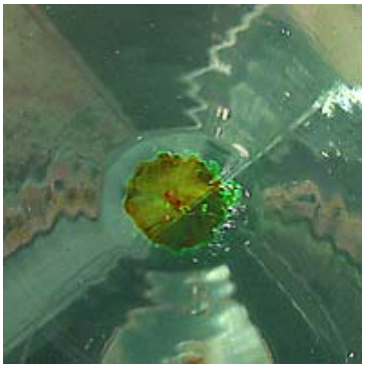
a)
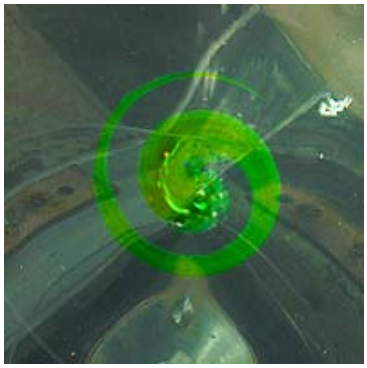
b)
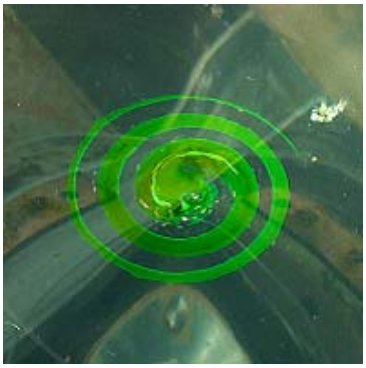
c)

Fig. 8. Spiral arm growing from the central uranil spot on the free surface: *a -c*) – $t =$ 0, 4, 6 s ($H =$ 40 cm, $\Omega =$ 200 RPM, $R =$ 7.5 cm).

The dye from the initial spot is transported inside the fluid involved in compound vortex motion along a vertical cylindrical surface (Fig. 9, a) of diameter 2.76 cm (diameter of central spot in Fig. 8, a is 3.01 cm). Dye from a growing spiral arm is transported inside along another cylindrical surface (Fig. 9, b) of diameter 7.39 cm. The second source starts to act later but the dye along the outer cylindrical envelope moves faster. When the round dye wall contacts with the boundary layer on the rotating disk the dye is extracted from the outer envelope and uniformly colour the whole volume (Fig. 9, d). The central dyed rod is saved during the mixing of dye from outer envelope.

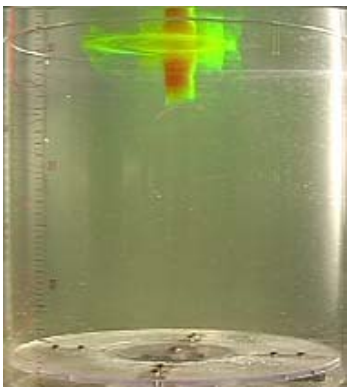
a)
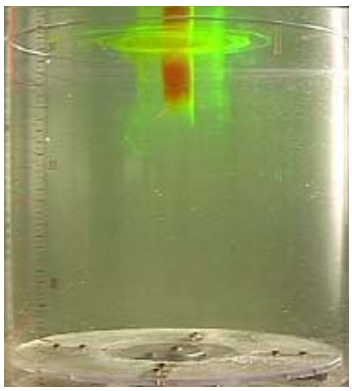
b)

c)

Fig. 9. Transport of the dye by compound vortex flow inside the fluid body: *a - c*) – $t =$ 18, 39, 114 s ($H =$ 30 cm, $\Omega =$ 200 RPM, $R =$ 5.0 cm).

Similar flow patterns that are spiral arms on the fluid surface and coloured cylindrical rods and envelopes are formed when the ink drop falls on the free surface. Due to partial shadowing by the dense ink dye the finest flow details are similar to ones described above, however, not so well distinguished.

CONCLUSION

Experiments performed in stratified and rotating fluids demonstrate that both wave and vortex flows have complex structure unifying large scale and small-scale components. To fix large-scale components a wide view instruments are used. To register small scale components sensitive instruments with a high spatial resolution are necessary. Character of mass transport depends on initial position of source in flow fields. In stratified flows stagnant blocked fluids and attractive high gradient interfaces are distinguished. In vortex flows dye from a compact source is accumulated in spiral domains and on cylindrical surfaces.

ACKNOWLEDGMENTS

The author would like to acknowledge partial financial support of the study provided by the Russian Academy of Sciences (Program “Dynamics of non-homogeneous fluids in external forcing fields”), the Ministry of Education and Science of the Russian Federation (Program “Support unique facilities”) and RFBR (grant 08-05-00473).

REFERENCES

Chashechkin, Yu.D. (1999), “Schlieren Visualization of a Stratified Flow around a Cylinder,” Journal of Visualization, **1**(4), 345-354.

Chashechkin, Yu.D. (2007), “Visualization of singular components of periodic motions in a continuously stratified fluid (Review report),” Journal of Visualization, **10(**1), 17-20.

Kistovich, A.V. and Yu.D. Chashechkin (2007), “Regular and singular components of periodic flows in the fluid interior,” J. Appl. Math. Mech. **71**(5), 762-771.

Maksoutov D.D. (1934), Tenevye metody issledovaniy opticheskikh system. Problemy noveyshoy Fisiki, vypusk XXIII. State Techn.-Theor. Publ., Leningrad-Moscow (In Russian). (Maksoutov D.D. Shadow methods of optic systems studying. Modern Physics Problems).

Chashechkin, Yu.D. and E.V. Stepanova, (2008), “Anisotropic Transport of an Admixture in a Compound Vortex,” Doklady Physics **53**(12), 634–638.